

Uniformity of radiation from a laser CRT based on a low-dimensional GaInP/AlGaInP structure with resonance-periodic gain

V.Yu. Bondarev, V.I. Kozlovsky, A.B. Krysa, Yu.M. Popov, Ya.K. Skasyrsky

Abstract. The metalorganic vapour phase epitaxy was used for growing GaInP/AlGaInP periodic structures with 25 quantum wells. The active elements based on these structures were prepared for a laser longitudinally pumped by a scanning electron beam. The structure is intended for resonance periodic gain in the case when the quantum wells are at the antinodes of the resonator mode corresponding to the peak of the gain line. The effect of the structural inhomogeneities over the thickness (up to 5%) on the lasing parameters is studied, as well as the temperature detuning from the resonant gain conditions. It is shown that the period of the structure must differ from the optimal value by no more than 0.7% for attaining a 10% uniformity in the lasing threshold along the active element.

Keywords: laser cathode-ray tube, A_3B_5 compounds, low-dimensional heterostructures.

1. Introduction

Laser cathode-ray tubes (CRTs) are promising sources of monochromatic light for display technologies [1, 2]. The use of low-dimensional structures as active elements considerably lowers the lasing threshold and improves other parameters of laser CRTs [3]. The parameters were improved by using a periodic structure with a relatively small (15–25) number of quantum wells (QWs) located at the antinodes of the resonator mode corresponding to the peak of the gain line [4]. Such laser structures used for optical pumping were called structures with resonant periodic gain [5]. However, the need for resonance tuning imposes more stringent requirements on the precision of their preparation. In particular, a departure of the structure from the optimal value would lead to an increase in the lasing threshold and a deterioration of other laser parameters. As a matter of fact, the structural period as well as the uniformity of layer thickness along the surface of the structure can be reproduced in real conditions only to

a certain degree of precision in different experiments. Layer thickness nonuniformity in laser CRTs may lead to an unacceptable spatial nonuniformity of lasing parameters along the active element.

In this work, we study the dependence of the main lasing parameters of the active element of a laser CRT prepared from a structure with resonant periodic amplification on the accuracy of coincidence of the QW position with the antinodes of the standing wave in the resonator. The obtained results are used to formulate the requirements imposed on the parameters of the structure for attaining the desired uniformity of the radiation emitted by the laser CRT.

2. Experiment

The structure to be investigated was prepared at the EPSRC National Centre for III-V Technologies, University of Sheffield, UK, by metalorganic vapour phase epitaxy (MOVPE) on a GaAs substrate disoriented by 10° from the (001) plane towards (111)A. The substrate was not rotated during epitaxial growth. The structure contained successively grown 1- μm thick GaAs buffer layer, a 6-nm thick $\text{Ga}_{0.5}\text{In}_{0.5}\text{P}$ layer, 25 pairs of 185-nm thick $\text{Al}_{0.35}\text{Ga}_{0.15}\text{In}_{0.5}\text{P}$ barrier layers and 8-nm thick $\text{Ga}_{0.5}\text{In}_{0.5}\text{P}$ QW layers, a 4.38- μm thick $\text{Al}_{0.35}\text{Ga}_{0.15}\text{In}_{0.5}\text{P}$ passive layer, and a 6-nm thick $\text{Ga}_{0.5}\text{In}_{0.5}\text{P}$ layer. The 6-nm thick $\text{Ga}_{0.5}\text{In}_{0.5}\text{P}$ layers were used to prevent the oxidation of the outer $\text{Al}_{0.35}\text{Ga}_{0.15}\text{In}_{0.5}\text{P}$ layers during the formation of the laser active element. The above thicknesses were obtained as a result of calculations. The barrier layer thickness was chosen so that the total optical thickness of the barrier layer and the QW layer was equal to the generation wavelength:

$$h_b N_b + h_{\text{qw}} N_{\text{qw}} = \lambda_g, \quad (1)$$

where h_b and h_{qw} are the thicknesses of the barrier layer and the QW layer, respectively; N_b and N_{qw} are the refractive indices of the barrier layer and the QW layer, respectively, at the laser wavelength λ_g . The data used in calculations were borrowed from [6, 7]: $N_b = 3.3$ and $N_{\text{qw}} = 3.6$ at $\lambda_g = 640$ nm. Figure 1 shows an image of the initial structure illuminated by a sodium vapour lamp. Interference fringes of constant thickness can be seen at the surface of the structure, which points towards its non-uniformity over the thickness. Five fringes are observed on the major part of the surface; hence the nonuniformity is approximately 5% for a total structure thickness of 9.2 μm .

V.Yu. Bondarev, V.I. Kozlovsky, Yu.M. Popov, Ya.K. Skasyrsky
P.N. Lebedev Physics Institute, Russian Academy of Sciences, Leninskii
prosp. 53, 119991 Moscow, Russia; e-mail: vikoz@mail1.lebedev.ru;
A.B. Krysa EPSRC National Centre for III-V Technologies, University
of Sheffield, UK

Received 17 June 2004

Kvantovaya Elektronika 34 (10) 919–923 (2004)

Translated by Ram Wadhwa

This nonuniformity was used to study the effect of detuning from resonance on the laser parameters. Three regions in which the laser parameters will be compared below are shown in Fig. 1.

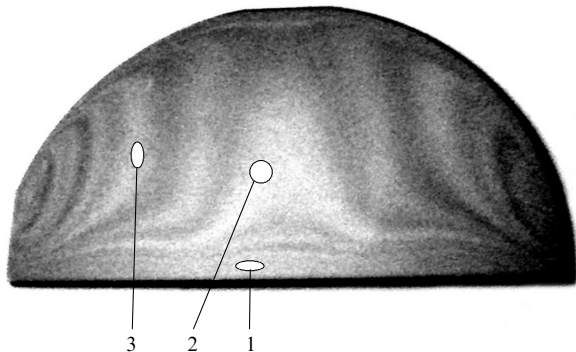


Figure 1. Image of the structure (half plate of diameter 50 mm) illuminated by sodium vapour lamp; 1, 2, 3 are regions for which the laser parameters are compared.

A semitransparent mirror formed by five pairs of quarter-wave layers $\text{SiO}_2/\text{TiO}_2$ and corresponding to a wavelength λ_g was first deposited on the growth surface of the structure. The theoretical value of the reflection coefficient for this mirror was 94%. The structure was then glued to a sapphire disk with the deposited surface downwards by using epoxy adhesive. The GaAs substrate was then polished mechanically to a thickness of 80 μm , while the remaining part of the substrate and the GaAs buffer layer were removed by selective etching in a solution of $\text{KOH}-\text{NH}_3\text{OH}-\text{H}_2\text{O}_2-\text{H}_2\text{O}$. The first thin layer of GaInP was a good stop-layer. Finally, a totally reflecting mirror containing 7.5 pairs of $\text{SiO}_2/\text{TiO}_2$ layers and a 0.1- μm thick Al layer was deposited on the free surface of the structure. The two mirrors formed an optical cavity whose length (9.2 μm) was equal to the structure thickness. The use of the SiO_2 layer with a lower refractive index as the first quarter-wave layer of the mirror ensured a nearly zero phase shift of the reflected wave at the mirror–structure interface. This is important for matching the positions of the QW with the antinodes of the standing wave in the cavity.

The laser parameters of the active element were studied in a dismantlable CRT. The active element was placed in a toroidal cryostat through which water could be circulated in addition to flushing of the liquid nitrogen vapour. In the case of water-cooling, the cryostat was connected to an external thermostat in which the water temperature could be stabilised in the range 14–100 $^\circ\text{C}$. The temperature in the cryostat was monitored by a copper–constantan thermocouple.

The active element was excited by a tightly focused electron beam. The half-amplitude diameter d_e of the electron spot at the active element surface was 25 μm for a total electron beam current $I_e = 200 \mu\text{A}$ and an electron energy $E_e = 40 \text{ keV}$. The spot diameter increased upon an increase in I_e and a decrease in the value of E_e . The parameters were studied in the pulse-scanning mode along a chosen line for $E_e = 25 - 60 \text{ keV}$ and $I_e = 0 - 2 \text{ mA}$. The length of the line was 2 cm, the pulse frequency was 50 Hz, and the scanning rate v_{sc} was $4 \times 10^5 \text{ cm s}^{-1}$. The current was measured by a tantalum slip ring calibrated by using a

Faraday cylinder. The laser emission spectrum was detected with a CCD array fabricated at the Institute of Spectroscopy, Russian Academy of Sciences. The CCD array was mounted at the exit of an MDR-4 spectrometer (LOMO). The power was measured with a calibrated FEK-29 photo element cell.

We also studied the cathode luminescence spectra at low level cw excitation levels and photoreflexion spectra of the initial structure. The emission spectrum for $E_e = 40 \text{ keV}$, $I_e = 1 \mu\text{A}$ and $d_e = 1 \text{ mm}$ corresponds to spontaneous emission. In both cases, we used an objective condensing the radiation beam in a solid angle $\sim 0.1 \text{ srad}$ in the vicinity of the normal to the growth surface of the structure.

3. Experimental results and discussion

The lasing spectrum of the active elements consisted mainly of one or two longitudinal resonator modes (depending on the position of the lasing region on the initial structure, see Fig. 1). In several cases, a jump of the laser wavelength by several mode intervals was observed. A typical example of such a hopping is presented in Fig. 2 which shows the lasing spectrum of region 3 (see Fig. 1) at a temperature $t = 95^\circ\text{C}$, $E_e = 40 \text{ keV}$, $I_e = 2 \text{ mA}$ and for different values of excess over the lasing threshold. The excess over the threshold was increased by decreasing the electron spot diameter from $\sim 1 \text{ mm}$ to 40 μm . One can see from Fig. 2 that much below the lasing threshold, the emission spectrum of the active element consists of several longitudinal modes of the resonator with the envelope peak at $\lambda = 648 \text{ nm}$ (lower spectrum). The shape of the envelope approximately corresponds to the spontaneous emission spectrum of the initial structure prior to the formation of the cavity. The intensity of one of the modes increases substantially at the generation threshold, and single-mode lasing is observed at a wavelength of 648 nm. However, a further decrease in the electron spot diameter leads to additional generation at a mode separated from the lasing line by four mode intervals towards the shortwave region. For a certain value of d_e , the intensities of the two lines become equal, but a further increase in the excitation level

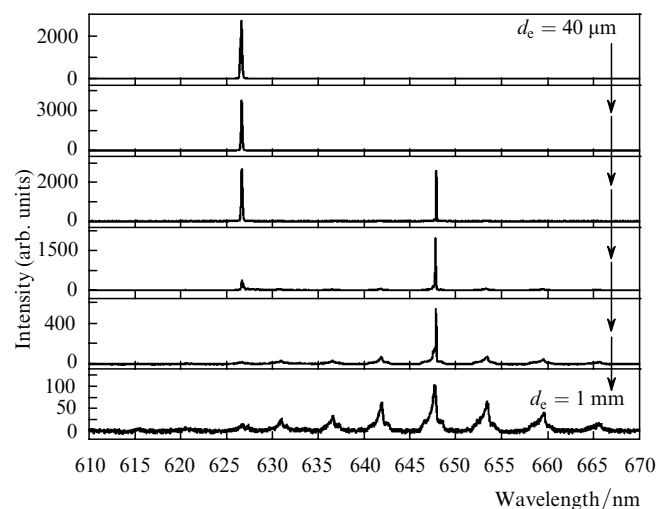


Figure 2. Laser emission spectra for region 3 (Fig. 1) for an electron spot diameter d_e varying from 40 μm (upper spectrum) to 1 mm (lower spectrum); $E_e = 40 \text{ keV}$, $I_e = 2 \text{ mA}$, and $t = 95^\circ\text{C}$.

(decrease in d_c) increases the intensity of the line corresponding to shorter wavelength $\lambda = 627$ nm.

Qualitatively, the observed hopping of the lasing wavelength can be explained by the fact that the period in the QW arrangement at the chosen structure region is shorter than the optimal period. In this case, the threshold conditions are attained first for the mode closest to the spectral peak of the amplification line, which corresponds approximately to the peaks of the spontaneous emission line for a relatively low level of excitation at room temperature. (To determine more precisely the peak of the amplification line, we must take into account the long-wave shift relative to the spontaneous emission peak due to renormalisation of the forbidden gap width, as well as the shortwave shift due to filling of the electron states in the allowed subbands of the QWs.) However, since the separation between the QWs is smaller than the gap between antinodes of the lasing mode of the resonator, only a part of QWs (about half in our case) participate in lasing.

In this connection, the concentration of nonequilibrium charge carriers in QWs, which are located near the nodes of the lasing mode of the resonator and practically do not participate in lasing, continues to increase as the pumping increases above the threshold value. This leads to a further increase in the gain at other wavelengths, in particular, on the shortwave side of the lasing line. As a result, lasing appears at a certain excitation level above the threshold value at a mode in which the separation between antinodes coincides with the separation between QWs. For lasing to occur in this matched mode, the optical gain in the QWs must be much lower than in the nearest neighbouring modes and about half the value for the first generated mode since the number of effectively operating QWs for the matched mode is twice as large.

The hopping of the lasing line upon an increase in the pump intensity at the same temperature $t = 95^\circ\text{C}$ was not observed in region 1 in Fig. 1, and single-mode lasing was observed for all pump levels. For this region, the structure period at the given temperature was close to the optimal value, thus making it possible to obtain the lowest possible generation threshold for the given structure (see Fig. 4 below). However, the optimal value of the structure period changes with temperature. This is due to the fact that the low-temperature dependences of the spontaneous emission peak (and hence the peak of the amplification line) differ considerably from the temperature dependence of the optical separation between two neighbouring QWs.

Figure 3 shows the photoreflection and cathode luminescence spectra of the region in the initial structure closest to region 3 in Fig. 1 at various temperatures. The photoreflection spectra have a characteristic modulation associated with interference of rays reflected from the structure surface and from the heteroboundary with the GaAs substrate as well as the singularity associated with additional Bragg's reflection due to the periodicity of the structure. The number of QWs participating in generation is the highest precisely in the vicinity of this singularity. In the general case, Bragg's reflection must affect the generation threshold. Estimates show, however, that since high-reflectivity mirrors ($R_1 R_2 = 0.94$) are used in our case, the Bragg reflection from the structure need not be taken into consideration. As the temperature changes from liquid nitrogen temperature to $t = 95^\circ\text{C}$, no significant changes are observed in the shape of the reflection spectrum, but the

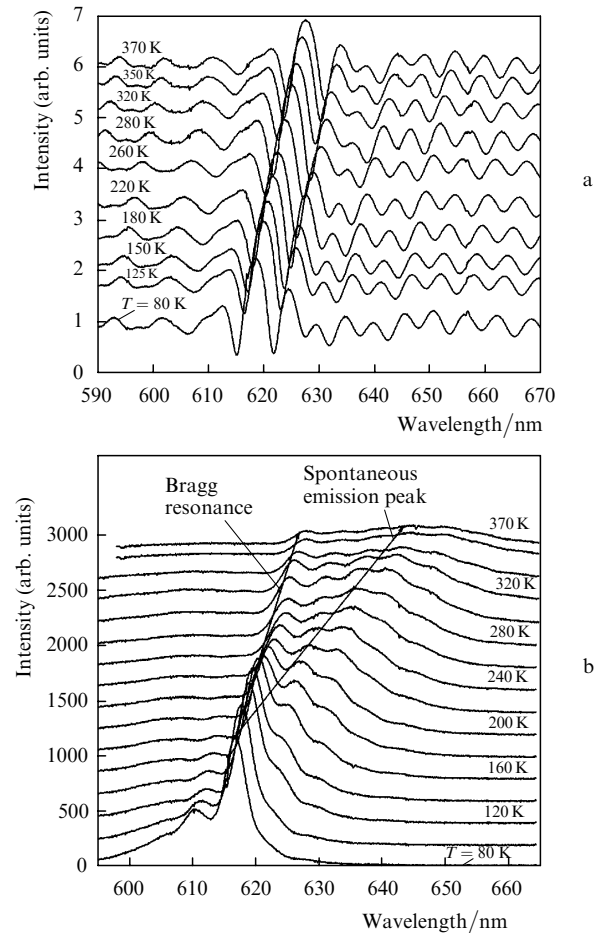


Figure 3. Photoreflection spectra in the vicinity of region 3 (a) and spontaneous emission spectra of the initial structure (b) at $T = 80 - 370$ K.

peak of the singularity is displaced towards the long-wave side at the rate of 0.31 nm K^{-1} .

The cathode luminescence spectra are also modulated due to interference of emerging rays, which is associated with the thickness of the structure and exhibit a singularity associated with Bragg's reflection from the structure. It can be seen that the local peak of the envelope of the cathode luminescence spectrum in the peak region of the spontaneous emission line is displaced upon heating towards the long-wave side at a much higher rate (approximately 0.092 nm K^{-1}) as compared to the singularity associated with Bragg's reflection. This difference in the temperature shifts of the emission line and Bragg's resonance leads to the temperature dependence of the optimal period of the structure.

Figure 4 shows basic dependences of the lasing parameters for the three regions indicated in Fig. 1 on the temperature of the active element. The symbols in Fig. 4a denote lasing modes, the dashed lines show the temperature variation of the Bragg resonance, and the solid line shows the temperature variation of the position of the spontaneous emission peak. It can be seen that at different temperatures lasing occurs in the vicinity of the peak of spontaneous emission and the Bragg resonance of the structure. If the Bragg resonance corresponds to a smaller wavelength, the intensity of the lasing mode in the vicinity of this resonance for highest excitation levels will be higher

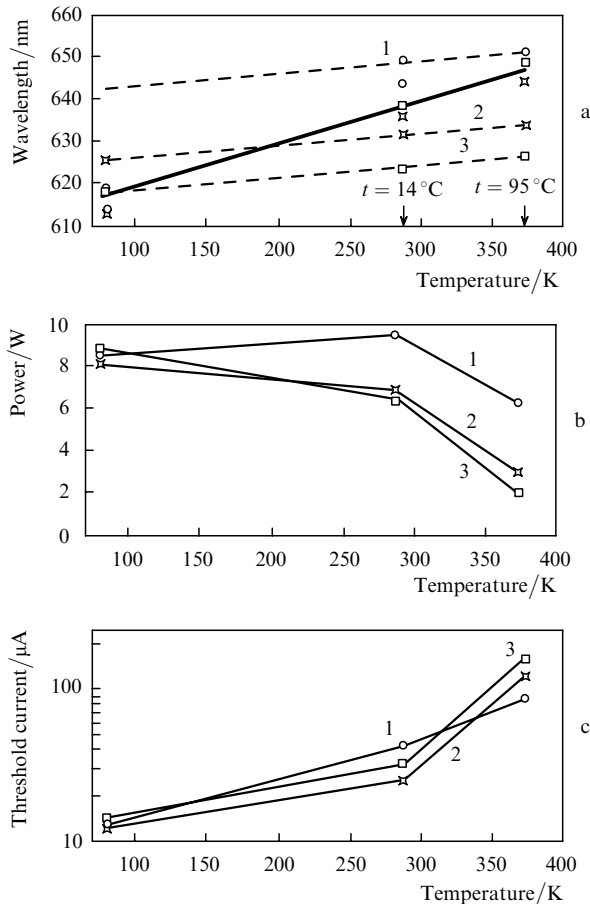


Figure 4. Spectral position of generation modes (a), lasing power at $I_e = 2$ mA (b), and threshold current (c) for structure regions 1, 2 and 3 (Fig. 1) at $T = 80, 287$ and 368 K; $d_c \approx 25$ μm for $I_e < 0.2$ mA and 40 μm for $I_e = 2$ mA and $E_c = 40$ keV. The bold solid line shows the temperature variation of the spontaneous emission peak of the initial structure, while the dashed lines show the temperature variation of the Bragg resonance for each region of the structure.

than in the vicinity of the spontaneous emission peak. The coincidence of the Bragg resonance with the spontaneous emission peak lowers the generation threshold at room temperature and at $t = 95^\circ\text{C}$. Indeed, the lowest threshold for $E_c = 40$ keV (Fig. 4c) is observed in region 2 at room temperature and in region 1 at $t = 95^\circ\text{C}$. The minimum values of threshold current $I_{th} = 25$ and 88 μA (current density $j_{th} = 8$ and 28 A cm^{-2}) were observed at $t = 14$ and 95°C , respectively. Such a low threshold at an elevated temperature (at $t = 95^\circ\text{C}$) has been attained for the first time. The generation threshold at the liquid nitrogen temperature is still lower and about the same for all three regions. This is due to the fact that the gain at low temperatures starts exceeding the blooming threshold quite rapidly, and hence the generation threshold is mainly determined by the blooming threshold.

Although lasing was achieved at room temperature in the entire investigated electron energy range ($E_c = 25$ – 60 keV), the highest generation efficiency was observed in the interval 40 – 50 eV. For these values of energy, the best depth matching of the excitation region with the active part of the structure was observed. Fig. 4b shows the temperature variation of the lasing power for $I_e = 2$ mA and $E_c = 40$ keV. Note that the lasing power depends not only on the generation threshold, but also on the generation

wavelength. For example, the highest lasing power at room temperature was attained in region 1 for a higher generation threshold than in regions 2 and 3. The power attained in this case was 9.5 W for a pump power transformation efficiency of about 12% , which is a record for lasers pumped longitudinally by an electron beam with such a low electron energy (40 keV). Moreover, the power dropped only to 6.2 W at $t = 95^\circ\text{C}$. The power decrease with increasing temperature was found to be much sharper for regions 2 and 3: from 6.8 to 3 W and 6.4 to 2 W, respectively, upon an increase in temperature from 14 to 95°C . The main reason behind such a decrease is the increase in the intracavity losses with temperature; this increase is especially sharp for generation at short-wave modes. These losses are apparently due to the edge absorption in AlGaInP barrier layers. Further studies must be carried out to solve this problem.

The lasing efficiency for region 1 is lower at low temperatures (80 K) than at room temperature. The Bragg resonance in this case is strongly displaced from the spontaneous emission line peak towards the long-wave region and lasing is observed in the vicinity of this peak. This means that only half of all QWs conditionally participate in lasing and transform the pump power into lasing power. The other half is overcrowded by carriers, most of which remain in the surrounding barrier layers. As a result, half the pump power remains unused and the intracavity losses associated with absorption of laser radiation by free carriers increase. Of course, some of the carriers diffuse to the operating QWs and a part of spontaneous radiation in overcrowded QWs and the barriers surrounding them is absorbed by the operating QWs and their barriers. For this reason, the lasing efficiency does not decrease as significantly as could be the case in the absence of these effects.

Figure 5a shows the dependence of threshold current on the departure of structure period from the optimal value at active element temperatures $t = 14$ and 95°C . The optimal value was chosen as the period for which the Bragg resonance of the structure coincides with the spontaneous emission peak. The curves drawn through the experimental points for each temperature have a minimum at the optimal value of the structure period. The horizontal lines correspond to the current exceeding the minimum threshold current by 10% . The vertical arrows corresponding to the intersection of these lines with the approximating curves define the range of variation of the structure period in which the threshold current does not exceed the minimum current by 10% . This range is 0.9915 – 1.0068 and 0.9926 – 1.0074 for $t = 14$ and 95°C , respectively. Thus, the total range is about 1.5% for both temperatures.

However, the output power of a laser is a more important parameter for a number of applications. Figure 5b shows the dependence of the lasing power on the departure of the structure period from the optimal value (relative to the threshold current) for $E_c = 40$ eV, $I_e = 2$ mA, and $t = 14$ and 95°C . One can see that the lasing power has no peak for the optimal period, which should be observed for a certain large structure period due to an increase in the generation threshold with the structure period. However, such a peak could not be observed in the structure studied here. It was mentioned above that the shift of the peak towards longer periods (wavelengths) is due to the spectrally dependent intrinsic losses in the barrier layers. In the range of the 10% variation of the threshold current (shown in

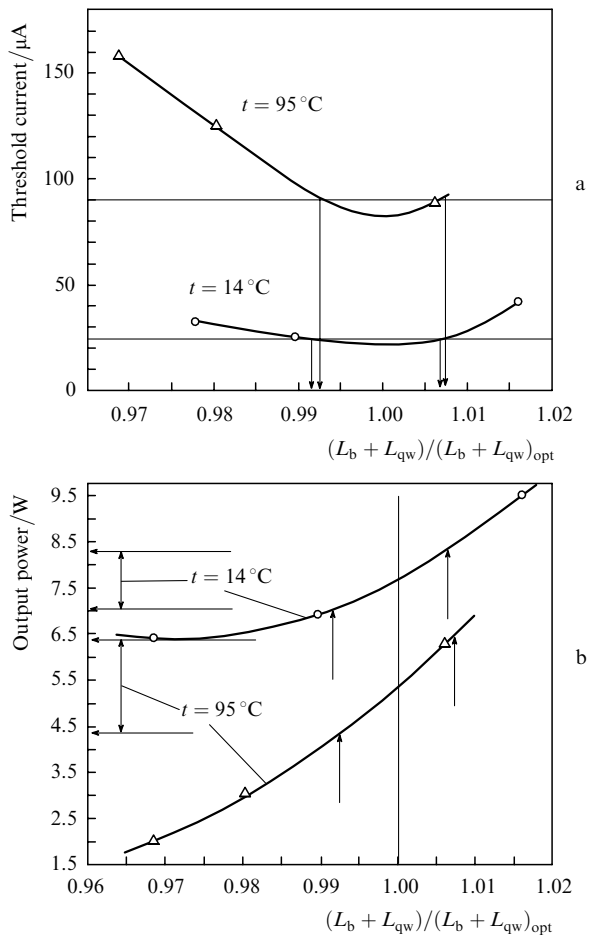


Figure 5. Dependence of the threshold current (a) and the output lasing power for $I_c = 2$ mA (b) on the departure of the structure period from optimal value corresponding to the threshold current minimum at $t = 14$ and 95°C for the same parameters as in Fig. 4. The horizontal lines in Fig. 5a show a 10% excess over the minimum threshold; the vertical arrows indicate the range of variation of the structure period for which the threshold exceeds the minimum value by not more than 10%. The vertical and horizontal arrows in Fig. 5b determine the range of variation of the lasing power corresponding to the range of structure variation for which the lasing threshold also exceeds the minimum value by no more than 10%.

Fig. 5b by vertical arrows), the lasing power changes by 17% and 38% at $t = 14$ and 95°C , respectively. It can be seen that the stabilisation of power requires a higher precision in the preparation of the structure. In addition, the structure optimisation is necessary for lowering the effect of absorption on lasing power.

4. Conclusions

The low-dimensional structures GaInP/AlGaInP with resonance-periodic gain make it possible to substantially improve the parameters of laser CRTs operating above room temperature. The lasing efficiency can be as high as 12% for an output power of 9–10 W at a wavelength of 643 nm at room temperature and at relatively low values of accelerating voltages (40–45 keV). However, the uniformity of laser CRT parameters along the active element surface depends to a considerable extent on the precision of structure preparation. To attain uniform lasing in threshold current of not worse than 10%, the period in the

arrangement of QWs along the working area of the structure should not differ by more than 0.7% from the optimal value (for a characteristic area of 4×3 cm). Power stabilization at room temperature requires a higher precision (approximately $\pm 0.5\%$). Such a precision is attainable on modern equipment used for MOVPE.

Acknowledgements. The authors thank John Roberts for his help in preparing the structure for investigations. This study was financed under the research programmes ‘Semiconductor Lasers’ and ‘Low-Dimensional Quantum Structures’ of the Russian Academy of Sciences, the Federal Programme ‘Physics of Solid-State Nanostructures’, Grant No. 04-02-16877 of the Russian Foundation for Basic Research, Project No. NSh-1466.2003.2 of the Research School, as well as by Principia Light Works Inc., CA, USA.

References

1. Kozlovskii V.I., Popov Yu.M. *Kvantovaya Electron.*, **33**, 48 (2003) [*Quantum Electron.*, **33**, 48 (2003)].
2. Tiberi M.D., Sherman G., Kozlovsky V.I. *SMPTE 143 Tech. Conf. and Exhibition* (New York, 2001) p.1.
3. Kozlovsky V.I., Korostelin Yu.V., Kuznetsov P.I., Krysa A.B., Skasyrsky Ya.K., Popov Yu.M. *Proc. XII Intern. Symp. «Advanced Display Technologies (FLOWERS'2003)»* (Korolev, Moscow Region, Russia, 2003) pp 33–36.
4. Bondarev V.Yu., Kozlovsky V.I., Krysa A.B., Roberts J.S., Skasyrsky Ya.K. *Intern. J. Nanoscience*, **3**, 193 (2004).
5. Raja M.Y.A., Brueck S.R.J., Osinski M., Schaus C.F., McInerney J.G., Brennan T.M., Hammons B.E. *IEEE J. Quantum Electron.*, **25**, 1500 (1989).
6. Mosel M., Winterhoff R., Geng C., Scholz F., Dornen A. *Appl. Phys. Lett.*, **64**, 235 (1994).
7. Kaneko Y., Kishino K. *Appl. Phys. Lett.*, **76**, 1809 (1994).